New Insights on the Mechanism of Palladium-Catalyzed Hydrolysis of Sodium Borohydride from ^{11}B NMR Measurements

G. Guella,* C. Zanchetta, B. Patton, and A. Miotello

Dipartimento di Fisica, Università degli studi di Trento, Via Sommarive 14, I-38050 Povo, Trento, Italy

Received: May 31, 2006; In Final Form: June 22, 2006

To gain insight on the mechanistic aspects of the palladium-catalyzed hydrolysis of $NaBH_4$ in alkaline media, the kinetics of the reaction has been investigated by ^{11}B NMR (nuclear magnetic resonance) measurements taken at different times during the reaction course. Working with BH_4^- concentration in the range 0.05−0.1 M and with a [substrate]/[catalyst] molar ratio of 0.03−0.11, hydrolysis has been found to follow a first-order kinetic dependence from concentration of both the substrate and the catalyst (Pd/C 10 wt %). We followed the reaction of $NaBH_4$ and its perdeuterated analogue $NaBD_4$ in H_2O, in D_2O and H_2O/D_2O mixtures. When the process was carried out in D_2O, deuterium incorporation in BH_4^- afforded $BH_{4-n}D_n^-$ ($n = 1, 2, 3, 4$) species, and a competition between hydrolysis and hydrogen/deuterium exchange processes was observed. By fitting the kinetics NMR data by nonlinear least-squares regression techniques, the rate constants of the elementary steps involved in the palladium-catalyzed borohydride hydrolysis have been evaluated. Such a regression analysis was performed on a reaction scheme wherein the starting reactant BH_4^- is allowed both to reversibly exchange hydrogen with deuterium atoms of D_2O and to irreversibly hydrolyze into borohydroxy species $B(OD)_4^-$. In contrast to acid-catalyzed hydrolysis of sodium borohydride, our results indicate that in the palladium-catalyzed process the rate constants of the exchange processes are higher than those of the corresponding hydrolysis reactions.

1. Introduction

The hydrolysis of sodium borohydride ($NaBH_4 + 4H_2O \rightarrow NaB(OH)_4 + 4H_2$) is of great practical significance in connection with hydrogen production to be used in fuel cells for energy supply in new portable and cellular technologies. This reaction is extremely efficient, because the total produced H_2 stems both from $NaBH_4$ (one-half) and from H_2O (the other half). Moreover, the H_2 thus generated is almost free of impurities, and it may be used in proton exchange membrane (PEM) fuel cells without further cleanup. To have practical significance in hydrogen production and power generation, the hydrolysis process of $NaBH_4$ must occur in such a way as to permit a controlled stability in hydrogen release.

Even if sodium borohydride is known as a hydrogen source via its hydrolysis, it can also be oxidized directly in an electrochemical cell when the eight-electron anodic process $BH_4^- + 8OH^- \rightarrow BO_2^- + 6H_2O + 8e^-$ is coupled to a suitable cathodic half-reaction such as $2O_2 + 4H_2O + 8e^- \rightarrow 8OH^-$. The calculated standard electromotive force of the overall working reaction $BH_4^- + 2O_2 \rightarrow BO_2^- + 2H_2O$ is 1.64 V, suggesting a strongly exergonic process[1] (calculated Gibbs free energy energy is -303 kcal mol^{-1}). Until now, however, the development of such a fuel cell is hampered by the poor utilization efficiency of the BH_4^- electroxidation due to the competitive hydrolysis leading to products which, in turn, are oxidizable at somewhat more negative potentials than the parent ion. Hydrogen evolution is considered here to be a major problem affecting the Coulombic efficiency of the system and the number of utilized electrons.[2]

* guella@science.unitn.it. Tel: +39 0461 88 1536. Fax: +39 0461 88 1696.

As opposed to other chemical hydrides, such as $LiAlH_4$ or NaH, only a small amount of hydrogen is liberated after borohydride dissolution in water (solid $NaBH_4$ and molar excess of water). In fact, the formation of strongly basic metaborate ion ($B(OH)_4^-$) leads to a fast pH increase of the solution and, thereafter, to a quenching of the overall hydrolytic process.[3] This outcome has been exploited to prepare concentrated aqueous solutions of $NaBH_4$ in strongly alkaline media where such a hydride is stable over a period of 6 months when stored under nitrogen at room temperature (half-life of 426 days at pH 14 and $T = 298$ K). Alkaline solutions of $NaBH_4$ can, however, be promptly hydrolyzed by using selected metal (or metal salts) catalysts, such as the transition metals Pt, Ru, Co, and Ni, eventually dispersed on different solid supports. In such a system, hence, the presence/absence of a suitable metal catalyst acts as an on/off switch for generation of H_2.

Even if the rate dependence on pH and other mechanistic details of the BH_4^- acid-catalyzed hydrolysis were deeply investigated by Schlesinger et al. more than 50 years ago,[3−5] the structures of true intermediates along the reaction pathway and the reaction variables controlling the competition between hydrolysis and exchange are still not fully understood.

The state of knowledge is even worse for metal-catalyzed BH_4^- hydrolysis where the true chemical nature of the catalyzing species (metal, metal boride, metal in oxidized form) is not definitely established, and more generally, the involved mechanism has been largely overlooked.

The overall hydrolysis reaction of borohydride, $BH_4^- + 3H_2O + H^+ \rightarrow B(OH)_3 + 4H_2$, takes place stepwise.[6] Besides the work of Mesmer and Jolly[7] (water solutions, pH range 3.8−14) and that of Wang and Jolly[8] (methanol−water solutions, low pH value: $[H_3O^+] = 0.1-1.1$ M, $T = 195$ K), most kinetic

10.1021/jp063362n CCC: $33.50
Published on Web 08/10/2006

studies were performed in alkaline or strongly alkaline solutions. There is a general agreement that, in these media, the loss of the first of four hydrogen atoms is the rate-determining step for the overall process.[9] In alkaline media, the attack on BH_4^- by the protic solvent (H_2O) is thought to afford a pentacoordinate "BH_5" intermediate, the existence of which has been recently demonstrated by both theoretical[10,11] and experimental investigations.[12] This short-lived intermediate may eventually evolve in two different directions, either relaxing back to borohydride (with H/D scrambling if the hydrolysis is carried in a deuterated solvent) or decomposing irreversibly to molecular hydrogen and $B(OH)_4^-$, possibly via a BH_3 intermediate. According to Kreevoy and Hutchins,[13] the values of the specific rate constants at $T = 298$ K for BH_4^- hydrolysis are $k_{H+} = (9.9 \pm 0.3) \times 10^5$ L mol^{-1} s^{-1} and $k_{H_2O} = (2.2 \pm 0.2) \times 10^{-7}$ s^{-1}, while the ratio between the specific rate of the two competitive processes causing the disappearance of the presumed intermediate BH_5 is (2.3 ± 0.3) L mol^{-1}. When the hydrolysis is carried out in deuterated water (D_2O), the corresponding values are $k_{D+} = (5.3 \pm 0.4) \times 10^5$ L mol^{-1} s^{-1} and $k_{D_2O} = (2.4 \pm 0.3) \times 10^{-8}$ s^{-1}, and the ratio between the processing responsible for the disappearance of BH_4D is (1.09 ± 0.04) L mol^{-1} leading to proton-specific isotope effect of 1.9 and to a water isotope effect of 9.0.

In principle, heterogeneous catalysis presents many advantages over homogeneous acid-catalyzed hydrolysis, because it is expected to be almost independent from the pH of the reaction medium, the catalyst would be reusable and, more important for application in hydrogen production, it could act as an on/off device. Kaufman and Sen[14] have studied the effect of some transition metals (Cu, Ni, and Co) and their salts by concluding that the overall hydrogen production in the presence of metal salts is both metal- and acid-catalyzed due to the fast H^+ production in their reduction by BH_4^- species. These results were in good agreement with the mechanism previously proposed by Holbrook and Twist,[15] which still represents a milestone in the metal-catalyzed hydrolysis of the borohydride ion.

We report here the kinetic results of the metal-catalyzed BH_4^- hydrolysis (rate law and activation energy) obtained by using 10 wt % Pd/C as catalyst. A preliminary investigation on such a system was carried out, by measuring the hydrogen evolution rate with volumetric and/or gas-chromatographic (GC) techniques at different temperatures. Such data proved to be very useful to plan a complete nuclear magnetic resonance (NMR) kinetic analysis that allowed us to follow the time dependence of all the long-living species involved in the reaction, not only within the BH_4^-/H_2O reacting system but also its deuterated analogues, such as BD_4^-/H_2O or BH_4^-/D_2O reaction systems. By best fitting of the time dependence of the ^{11}B NMR signals, for the first time we report here the rate constants of the deuterium incorporation processes into initial borohydride and the corresponding hydrolysis specific rates. In fact, by using NMR, the expected competition between hydrolysis and hydrogen/deuterium exchange processes is promptly detected by the appearance, at different times, of all the deuterated hydrides $BH_{4-n}D_n^-$ ($n = 0, 1, 2, 3, 4$). The adopted simulation procedure involves the numerical solutions of the appropriate differential equations to account for a given reaction scheme in which the starting reactant BH_4^- is either allowed to reversibly exchange its hydrogen with deuterium atoms of D_2O and to irreversibly hydrolyze (together with the above-mentioned partially deuterated hydrides) to borohydroxy species $B(OD_4)^-$.

2. Experimental Methods

2.1. Reagent and Sample Preparation. An alkaline solution of sodium borohydride (pH 13, (0.055 ± 0.001) M; Carlo Erba Reagents), was prepared for GC measurements. Alkaline solutions (10 mL, pH 13) of sodium borohydride and sodium borodeuteride (Sigma Aldrich Reagents) were prepared for each of four sets of NMR experiments: solution 1, $NaBH_4/H_2O$ (0.073 ± 0.002) M; solution 2, $NaBH_4/D_2O$ (0.057 ± 0.002) M; solution 3, $NaBD_4/H_2O$ (0.088 ± 0.002) M; and solution 4, $NaBD_4/D_2O$ (0.085 ± 0.002) M; by dissolving the suitable amount of solid sample in 0.10 M NaOH or 0.10 M NaOD. The latter was obtained by deuterium exchange of dry solid NaOH and repeated treatments with D_2O (99.9%, Merck). The titer values of reagents were independently measured through iodometric method.[4]

Kinetic measurements, aimed at establishing the rate law of the BH_4^-/H_2O, in Pd/C 10 wt %, were carried out by following the H_2 evolution rate by GC analysis, adding, respectively, 79.82 (0.0015 M), 159.63 (0.0030 M), 239.45 (0.0045 M), and 319.26 (0.0060 M) mg of commercially available Pd/C (Sigma-Aldrich, Milano) to 50 mL samples of the above solutions ((0.055 ± 0.001) M) with 150 mL of distilled water.

NMR measurements were carried out by adding, respectively, 6.0, 6.4, 7.5, 6.3, and 5.9 mg of commercially available Pd/C (10 wt % Sigma-Aldrich, Milano) to the borohydride solutions 1−4 prepared as previously described. To avoid systematic errors, all the NMR measurements were carried out at least in duplicate.

For each set of NMR measurements, 500 μL of $NaBH_4$ or $NaBD_4$ alkaline solutions (pH 13) were put into a 5 mm NMR test tube. In the $NaBH_4/H_2O$ and $NaBD_4/H_2O$ runs, the samples were added with 50 μL of D_2O to provide an internal lock frequency control. All the NMR instrumental parameters were optimized for both ^1H and ^{11}B detection, and a reference spectrum was always acquired before the addition of the catalyst.

2.2. GC Measurements. The rate of hydrogen emission was evaluated by GC measurements carried out with Agilent 3000 Micro GC (Agilent Technologies) equipped with a Plot-U (3 m) and a molecular sieve (10 m) columns.

An appropriate reactor with a thermostatic bath was used for the reaction study. The system was set up to permit the connection with other devices used in the experiment (pressure sensor, inlet gas, catalyst insertion device) and to collect emitted hydrogen to the GC instrument. In any run, the catalyst was placed on the appropriate device inside the reactor, and the system was sealed. Nitrogen was used as a feed gas (20 kPa), acting also as the solution stirrer. This configuration permitted a response time of GC of approximately 1 min. To avoid gas condensation in the inlet tube of GC, a water vapor trap was placed on the gas evolved line; argon was used as the gas carrier (0.55 MPa).

To follow the hydrogen evolution during reaction, only a small portion of the produced gas must enter the GC device (about 1% of the total flow) which provided the rate of reaction in arbitrary units. Since a constant volume of the sampling gas is injected into the Micro GC at different times, the time dependence of the amount of detected hydrogen provides the evolution rate (in arbitrary units) of the reaction. With the concentration of the borohydride running solution before and after the end of reaction, a correct quantitative scale unit can be obtained and therefore the total amount of the produced hydrogen.

The amount of borohydride present in the system was determined by the use of the iodometric method[4] by adding a

molar excess of IO_3^- to the reaction medium and back-titrating the remaining IO_3^- with buffered $S_2O_3^{2-}$.

2.3. NMR Measurements. NMR spectra were taken at 298.2 K with an Avance 400 Bruker spectrometer operating at 400.13 MHz for ^1H and at 128.38 MHz for ^{11}B and equipped with a 5 mm inverse broad band (BBI) probe. δ_B values were recorded in parts per million (ppm) relative to $BF_3{\cdot}Et_2O$ ($=$0.0 ppm in $CDCl_3$) and δ_H values relative to the solvent residual signals (δ_H 4.72 ppm). Optimized $\pi/2$ pulse width for ^1H (8 μs, at a transmission power of 0.0 dB) and ^{11}B (12 μs, at a transmission power -3.0 δ_B) were obtained on the same samples by the Bruker subroutine. The length of the $\pi/2$ pulse was checked at the beginning of any measurement session, and the temperature was controlled throughout the experiments to $\pm$0.1 K. ^1H NMR spectra were taken by using water suppression pulse sequence, while ^{11}B NMR spectra were acquired either as fully coupled or as proton-decoupled with 5 s time delay: 32 scans. The phase-cycled Hahn echo pulse sequence[16] was also used with a recycle time of 2 s, delay between pulses was 100 ms, sweep width was 38.46 kHz, and acquisition time was 0.104 s. In all ^1H and ^{11}B NMR measurements, 32k data points were collected leading to a digital resolution of 0.28 Hz/point (SWH $=$ 9260 Hz) and 0.25 Hz/point (SWB $=$ 8280 Hz), respectively. Data were collected with *XWINNMR* (version number 1.3) and processed using both Bruker *TOPSPIN* (version number 1.3) and *MestReC* data processing software.[17]

^1H, $^{11}B-^1H$ coupled, or $^{11}B-^1H$ decoupled experiments could in principle be used for our purpose, but we decided to rely on the latter hardware configuration and to use the Hahn echo pulse sequence for reducing rolling baselines of the NMR spectra. With such a pulse sequence, the multiplicity of all the $BH_{4-n}D_n^-$ (n $=$ 1, 2, 3, 4) species could be better detected, and the area of the corresponding signal at any given time more easily integrated.

Due to the low magnetic moment of Pd atoms (-0.642 μ/μ_n), the relaxation times of ^1H and ^{11}B NMR signals are not significantly affected by the presence of metal in the analyzed sample. Moreover, even if at the beginning of the reaction the magnetic field homogeneity is lowered by H_2 bubbling off and by the inhomogeneous character of the sampled solution, NMR spectra with acceptable resolution can be taken through kinetic runs.

In borohydrides and their hydroxy derivatives, the majority of the chemical shifts of ^{11}B (H coupled) signals occur between 10 and -50 ppm (assuming $BF_3{\cdot}Et_2O$ as reference at 0.0 ppm), which represent a span of about 8000 Hz at the operating instrumental frequency, whereas the J values of the $^{11}B-^1H$ coupling are about 80 Hz. Since the line width of ^{11}B NMR signals is quite narrow and the chemical shift of the hydrolysis intermediates $BH_n(OH)_m$ is expected around $0-20$ ppm, the ^{11}B spectra provide sufficient information for the determination of individual structures.

2.3.1. Procedure During Kinetics Measurements. The initial time of the reaction was taken after addition, through a homemade minifunnel, of a suitable amount of the catalyst powder ($\sim$10% on molar ratio). The sample tube was then strongly shaken and introduced into the NMR probe, the field homogeneity rapidly optimized, and a multiple acquisition experiment launched. The elapsed time between catalyst addition and the first NMR spectrum acquisition was always in the range $90-110$ s. Since the spin$-$lattice (T_1) relaxation times of the ^{11}B nucleus in the borohydrides (no matter their H/D label) are significantly longer (about 12 s) than T_1 of borates $B(OH)_4^-$/$B(OD)_4^-$ (about 1 s), the empirical integration constant for the former was evaluated before the addition of the catalyst and for the latter at the end of the reaction. They were, hence, consistently used for all the spectra collected throughout. After the catalyst particle precipitation, the solution contained in the main volume sampled by the RF coil becomes almost homogeneous.

2.3.2. Data Analysis. To fit the time dependence of all the chemical species detectable by NMR, the disappearance of the hydride BH_4^- (and of its deuterated analogues) and the increase of the borate $B(OH)_4^-$ were followed and analyzed. The major work was carried out on the BH_4^-/D_2O system wherein all the intermediate species $BH_{4-n}D_n$ (n $=$ 0, 1, 2, 3, 4) and the hydrolysis end product $B(OD)_4^-$ were detected.

To follow the evolution of whole system, only the central peak of any species was considered. Due to the spin quantum number of deuterium (I $=$ 1), BH_4^- appears in the ^{11}B-proton-decoupled spectrum as a singlet, BH_3D^- as a 1:1:1 triplet (J_{B-D} $=$ 12.2 Hz), $BH_2D_2^-$ as 1:2:3:2:1 quintet, BHD_3^- as a 1:3:6:7:6:3:1 septet, and BD_4^- as a 1:4:10:16:19:16:10:4:1 nonet (see Figure 1). Therefore, to normalize the integrated signals, the area was multiplied for a suitable factor (by referring to the species $BH_{4-n}D_n$, such a factor is 1, 3, 3, 27/7, and 81/19 for n $=$ 0, 1, 2, 3, and 4, respectively).

The integration of single peaks involved signal deconvolution due to the peak overlap. Every spectrum was phase-optimized in a frequency domain nearby the interested peak.

2.3.3. Simulation and Fitting. All NMR data have been used as input data for the *Gepasi* program, a free software for the simulation of the dynamics of chemical processes,[18-20] using a Levenberg$-$Marquardt fitting optimization model. The software converts the whole set of equations defined by a given reaction scheme in a matrix system of differential equations.

Gepasi uses the sum of squares of residuals

$$\mathrm{ssq} = \sum_i \left(\frac{y_i - y_i^*}{w_i} \right)^2 \qquad (1)$$

where the sum is over all the experimental data, y_i are the measured values of the variables, y_i^* are the simulated values of the variables, and w_i are weighting constants used to scale all variables to similar values such that all have equal weight on the fit. The global minimum of the sum of squares represents the best that the model can do to explain the experiment.

2.3.4. Ab Initio Calculations. Ab initio quantum chemical calculations were performed by using the *Gaussian 03* (revision C.02) package.[21] Geometry optimizations were carried out at the density functional theory level by using the hybrid functional DFT-B3LYP[22] and the 6-311++G(d,p) basis set. All structures were characterized by frequency calculations at the same level of theory in order to find stationary points as true minima (number of imaginary frequency $=$ 0), and zero point energy (ZPE) corrections were scaled by 0.9806, as usually performed at such a level of theoretical approach.[23]

3. Results and Discussion

3.1. GC Measurements. Commercial 10 wt % Pd/C powders were found to be efficient catalysts for the hydrolysis of sodium borohydride as shown in Figure 2, where the percentage of H_2 volume generated during the catalytic hydrolysis of 0.055 M $NaBH_4$ solution (pH 13) with different catalyst concentrations at T $=$ 296 K is reported. The hydrogen production starts immediately without any induction time and shows a first-order kinetic dependence on Pd concentration.

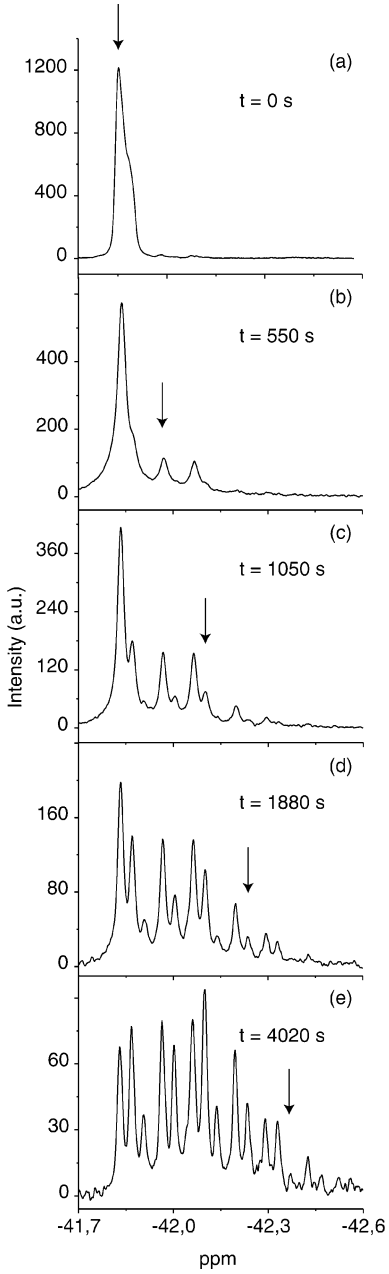

Figure 1. ^{11}B NMR proton-decoupled spectra taken at different times during the Pd/C catalyzed hydrolysis of solution 2. (a) Before the catalyst addition (singlet for BH_4^- species); (b) after 550 s (triplet for BH_3D^- species); (c) after 1050 s (quintet for $BH_2D_2^-$ species); (d) after 1880 s (septet for BHD_3^- species); and (e) after 4020 s (nonet for BD_4^- species). Arrows show the central peak of any multiplet.

Hydrogen evolution data can be nicely fitted in any run by a single exponential of the form $[H_2]_i(t) = [H_2]_{max}(1 - e^{-k_{obs,i}t})$ where $[H_2]_{max}$ is assumed from the reaction stoichiometry to be $[H_2]_{max} = 4[BH_4^-]_0$ and $k_{obs,i}$ represents the actual value of the rate constant observed for a given initial condition. In all the measurements carried out with an initial molar ratio of $[BH_4^-]/[Pd]$ within the range 0.03−0.11, we obtain first-order kinetics both in catalyst and in borohydride. We are well aware that the catalyst's activity depends on the Pd active sites on the surface of the C powder, but in a well-stirred dispersion of Pd/C catalyst, we can consider them to be proportional to the catalyst's "concentration", here written as [Pd]. To give an example, the value of k_{obs} in the run where Pd/C was present at 5.5% molar ratio was estimated to be $k_{obs} = (2.4 \pm 0.3) \times 10^{-4}$ s^{-1}.

We must emphasize that in the absence of catalyst the rate

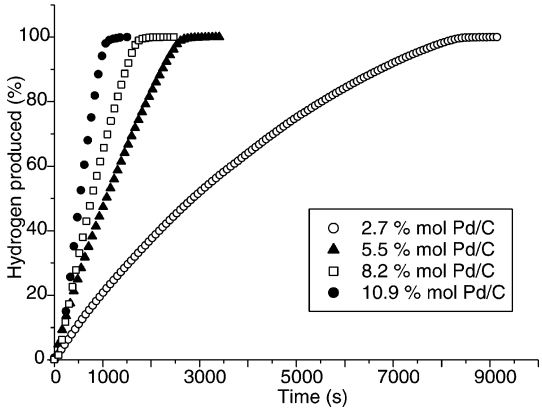

Figure 2. Hydrogen production versus time at different molar concentrations of metal catalyst.

constant evaluated according to Kreevoy and Hutchins at pH 13 would be[13] $k_{hyd} = k_{H+}[H_3O^+] + k_{H_2O}[H_2O] = 2.3 \times 10^{-7}$ s^{-1}. Hence, with our present catalyst amount, the overall catalytic effect is estimated to be about 4 orders of magnitude greater.

To obtain a rough estimate of the activation energy involved in the H_2 production, the values of the rate constant were determined at various temperatures. The slope of ln(*k*) versus the reciprocal absolute temperature (1/*T*) leads to an activation energy of 28 kJ mol^{-1}. This value is similar to the activation energy found by Amendola (47 kJ mol^{-1})[24] at higher $NaBH_4$ and NaOH concentrations and by Kaufman and Sen[14] with different bulk metal catalysts: 75 kJ mol^{-1} for cobalt, 71 kJ mol^{-1} for nickel, and 63 kJ mol^{-1} for Raney nickel.

Recently, an activation energy of 28.5 kJ mol^{-1} has been reported using Ru(0) nanoclusters[25] as catalyst. However, it must be emphasized that in such investigation a zero-order reaction process is observed as a function of the catalyst concentration. This reaction order is probably due to the BH_4^--induced dynamic saturation of the active sites of the catalyst surface during the reaction. Saturation effects are expected when hydride/catalyst molar ratio is high (always greater than 100) as in the case of Ru(0). On the contrary, in our measurements, such a ratio was never less than 40.

3.2. NMR Measurements. *3.2.1. NMR Kinetic Measurements with $NaBH_4$ in Alkaline H_2O.* In a typical ^{11}B-proton-decoupled NMR spectrum, obtained during hydrolysis (solution 1), aside from the upfield signal at −41.8 ppm, due to the unreacted BH_4^-, a broad signal at 1.76 ppm attributable to borate species $B(OH)_4^-$ was present. However, no intermediates of $H_nB(OH)_{4-n}^-$ (n = 1, 2, 3) type were detected. In principle, the lack of detection of such species could be due to the low symmetry of their structures leading to a significant broadening of ^{11}B signals. We must emphasize, however, that we were able to detect them during the acid-catalyzed hydrolysis of sodium borohydride (data not shown). In particular, the species BH_3OH^- was there found as a sharp 1:3:3:1 quartet (at −12.9 ppm, $J(^1H, ^{11}B) = 87.50$ Hz) in the fully coupled ^{11}B NMR spectrum. Since such a species (and/or any of the type $H_nB(OH)_{4-n}^-$) was not detected in the corresponding NMR spectra of the palladium-catalyzed hydrolysis, we conclude that they are not long-living intermediates along the coordinate of the Pd-catalyzed reaction. The observed rate constants of such a process were evaluated by following the time dependence of both BH_4^- and $B(OH)_4^-$ NMR signals and by fitting such experimental data with the Levenberg−Marquardt model as implemented in the *Gepasi* program. By fitting the NMR curves describing the time dependence, for a given amount of added catalyst, we found

two single-exponential functions of the form $[BH_4^-](t) = [BH_4^-]_0 e^{-k_{obs}t}$ and $[B(OH)_4^-](t) = [BH_4^-]_0[1 - e^{-k_{obs}t}]$. Such functions stem by integration, with suitable boundary conditions, of the first-order rate equations of the form $-d[BH_4^-](t)/dt = k_{obs}[BH_4^-](t)$ and $d[B(OH)_4^-](t)/dt = k_{obs}([BH_4^-]_0 - [BH_4^-](t))$. Thus, the value of $k_{obs,NMR}$ ($(3.6 \pm 0.2) \times 10^{-5}$ s^{-1} M^{-1}) (solution 1) can be straightforwardly obtained by simulation of the experimental curves. Such a value of $k_{obs,NMR}$ includes not only the true hydrolytic constant k_{hyd} but also the concentrations of catalyst (0.010 M). The true hydrolytic rate constant k_{hyd} (s^{-1} M^{-2}) of the BH_4^-/H_2O reacting system is therefore evaluated to be 3.6×10^{-3} s^{-1} M^{-2}. The first-order dependence of the rate from the BH_4^- concentration was confirmed by $t_{1/2}$ NMR measurements taken on samples containing different initial concentration of the hydride evaluated by the crossing point of the $BH_4^-(t)$ and $B(OH)_4^-(t)$ curves, observed at (340 ± 5) s.

No matter how the hydrolytic rate constant is evaluated, its value represents the true rate constant of the hydrolysis in pure water only if we could assume that the overall kinetic effect of the deuterated water (10 vol %), present in the NMR tube, is negligible. Since during the reaction course we do not observe any deuterium incorporation into BH_4^- species and the rate constant of the BH_4^- hydrolysis in D_2O is expected to be lower than in H_2O, the contribution of the second term ($k_{D_2O}[BH_4^-][D_2O][Pd]$) in the appropriate differential equation (see Supporting Information, eq 1) would be negligible. In fact, k_{D_2O} is about 4 times lower than k_{H_2O}, as will be discussed in the next section, and $[D_2O]$ here is 10 times lower than H_2O. Thus, the value of the true k_{hyd} of BH_4^- in $H_2O/D_2O = 9{:}1$ at any given initial ratio of borohydride/catalyst must be nearly the same, within the estimated relative error, as that of BH_4^- in pure H_2O at the same $[BH_4^-]$/[catalyst] ratio.

3.2.2. NMR Kinetic Measurements with $NaBH_4$ in Alkaline D_2O. a. Experiments. As expected and already anticipated (Figure 1), things are much more complicated when the hydrolysis is carried out in deuterated water (solution 2). In fact, in the upfield region of ^{11}B-proton-decoupled NMR spectrum, many other signals arise. In particular, deuterium incorporation in BH_4^- leads to $BH_{4-n}D_n^-$ ($n = 1, 2, 3, 4$) species which appear on the scene one after another. Besides the expected signal of unreacted BH_4^- and $B(OD)_4^-$ (singlets at δ_B −41.8 and 1.76, respectively), we detected here the presence of the deuterated species BH_3D^- (triplet at δ_B −42.0), $BH_2D_2^-$ (quintet at δ_B −42.2), BHD_3^- (septet at δ_B −42.4), and even traces of BD_4^- (nonet at δ_B −42.6). As already found in hydrolysis of solution 1, the scrambled intermediates $H_nD_mB(OD)_p^-$ ($n + m = 4 - p$; $p = 1, 2, 3, 4$) were not detected.

To estimate the rate constants of all the processes leading to scrambled hydrides and to the final $B(OD)_4^-$ species, the initial conditions must be accurately defined. This is not a simple matter when working with D_2O solutions, since heavy water in contact with air containing light water vapor rapidly becomes contaminated with it. Kobayashi[26] investigated the speed of this process and found that a sample of D_2O open to the air, at 294.5 K and 70% humidity, went from an initial 97.7% D to 13% in about 10 h. There is also an apparently rapid equilibrium, $H_2O + D_2O \rightleftharpoons 2HDO$, so that, after a few hours, only an equilibrated mixture among different isotopically substituted water molecules is formed. It follows that there is some uncertainty in the definition of D_2O and HDO initial concentrations. Since our experiments were carried out just after the preparation of solution 2, which was kept at $T = 277$ K in a closed vial, we can safely assume that the D_2O titer could be about 4% lower than that contained in the commercial sealed ampule (99.5%).

TABLE 1: Kinetic Constants, at 298 K, Obtained from the Simplified Model, According to the Reported Reaction Scheme[a]

rate constant	reaction scheme	values $\times 10^{-3}$ [s^{-1} M^{-2}]
$k_{1,hyd}$	$BH_4^- + D_2O \rightarrow B(OD)_4^- + HD$	(1.46 ± 0.04)
$k_{2,exc}$	$BH_4^- + D_2O \rightarrow \sum BH_{4-n}D_n^- + HDO$	(2.37 ± 0.07)
$k_{-2,exc}$	$\sum BH_{4-n}D_n^- + HDO \rightarrow BH_4^- + D_2O$	(11.7 ± 0.9)
$k_{3,hyd}$	$\sum BH_{4-n}D_n^- + D_2O \rightarrow B(OD)_4^- + HD$	(0.18 ± 0.02)

[a] $[D_2O] = 52.7$ M; $[HDO] = 2.5$ M.

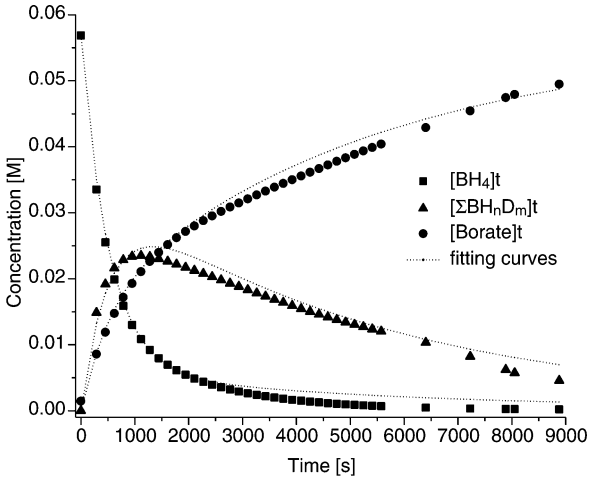

Figure 3. Consecutive irreversible first-order reaction. Dashed lines: fitting curves. Symbols: experimental data.

This assumption was roughly confirmed by comparison of the area of the HDO ^1H NMR signal in our BH_4^-/D_2O reacting system with respect to the area of the same signal in the same volume of the commercial sealed ampule. Such measurements lead to an estimation of HDO concentration in our sample of 2.5 M (and thus, D_2O is estimated to be 52.7 M). Both such concentrations are so high with respect to the initial BH_4^- concentration to ensure a pseudo-first-order kinetics for all the processes where they are involved. Since the equilibrium constant of the reaction $H_2O + D_2O \rightleftharpoons 2HDO$ is about 1, the residual $[H_2O]$ is expected to be absolutely negligible. Both in hydrolytic and in exchange processes, HDO may act either as a proton donor molecule (affording hydrolysis and exchange on all the scrambled hydrides but not on the initial BH_4^- species) or as a deuteron donor (affording hydrolysis and exchange on all the scrambled hydrides but not on the end products $B(OH)_4^-$ species). However, because $[D_2O]$ is about 25 times higher than [HDO] and the corresponding hydrolytic rate constants k_{hyd,D_2O} are not more than 5 times lower than $k_{hyd,HDO}$, the contribution to hydrolysis of the terms such as $k_{hyd,HDO}[HDO]$ should be about 5 times lower than terms such as $k_{hyd,D_2O}[D_2O]$. Concerning the effect on the H/D exchange, we can assume $k_{exc,HDO}$ to be almost the same as k_{exc,D_2O} in all the processes where HDO acts as a deuteron donor, while $k_{exc,HDO}$ must be evaluated in all the processes where HDO acts as a proton donor.

b. Results for Nonlinear Regression Analysis. A nonlinear least-squares regression technique was used to compare the experimental data with a simplified kinetic model (reaction scheme in Table 1) wherein we considered only the starting reactant (BH_4^-), the end product ($B(OD)_4^-$), and the global change of all the intermediate scrambled hydrides ($BH_{4-n}D_n$ with $n = 1, 2, 3, 4$). The "best fit" of the NMR data (see Figure 3) with the solutions of the differential equations (see Supporting Information, eqs 5−10) led to the best values of the hydrolysis (k_{hyd}) and exchange rate constants (k_{exc}) as reported in Table 1.

TABLE 2: Kinetic Constants at 298 K Obtained from Optimized Model[a]

rate constant	reaction scheme	values $\times 10^{-3}$ [s^{-1} M^{-2}]
$k_{1,hyd}$	$BH_4^- + D_2O \rightarrow B(OD)_4^- + HD$	(1.29 ± 0.09)
$k_{2,exc}$	$BH_4^- + D_2O \rightarrow BH_3D^- + HDO$	(2.9 ± 0.1)
$k_{-2,exc}$	$BH_3D^- + HDO \rightarrow BH_4^- + D_2O$	(27 ± 2)
$k_{3,hyd}$	$BH_3D^- + D_2O \rightarrow B(OD)_4^- + HD$	(0.4 ± 0.3)
$k_{4,exc}$	$BH_3D^- + D_2O \rightarrow BH_2D_2^- + HDO$	(1.2 ± 0.1)
$k_{-4,exc}$	$BH_2D_2^- + HDO \rightarrow BH_3D^- + D_2O$	10^b
$k_{5,hyd}$	$BH_2D_2^- + D_2O \rightarrow B(OD)_4^- + HD$	(0.3 ± 0.6)
$k_{6,exc}$	$BH_2D_2^- + D_2O \rightarrow BHD_3^- + HDO$	(1.6 ± 0.4)
$k_{-6,exc}$	$BHD_3^- + HDO \rightarrow BH_2D_2^- + D_2O$	9^b
$k_{7,hyd}$	$BHD_3^- + D_2O \rightarrow B(OD)_4^- + HD$	0.8^b
$k_{8,exc}$	$BHD_3^- + D_2O \rightarrow BD_4^- + HDO$	1^b
$k_{-8,exc}$	$BD_4^- + HDO \rightarrow BHD_3^- + D_2O$	10^b
$k_{9,hyd}$	$BD_4^- + D_2O \rightarrow B(OD)_4^- + D_2$	0.8^b

[a] The reaction scheme is reported in second column. $[D_2O] = 52.7$ M, $[HDO] = 2.5$ M. [b] Only indicative value.

The most interesting outcome is the prevalence of the exchange routes on the net hydrolytic reaction, at least in the early part of its evolution (0−20 min). Thus, in Figure 3, there is clear-cut evidence that the rate of overall formation of the scrambled intermediates is higher than the overall rate of formation of the hydrolytic end product $B(OD)_4^-$, which in turn is determined by D_2O attack on both BH_4^- and intermediate hydrides. In particular, the rate constants of the backward exchange reactions ($k_{-2,exc}$) have been found to be 5 times higher than that of the corresponding forward processes ($k_{2,exc}$); the latter, in turn, is about twice the hydrolytic rate constant of the BH_4^- species ($k_{1,hyd}$) and about 1 order of magnitude higher than the hydrolytic rate constants of all the deuteron-containing $BH_nD_m^-$ species ($k_{3,hyd}$).

The values of the rate constants obtained in such a simplified model were used as initial trial parameters in a more detailed reaction scheme (second column of Table 2) where we considered the reactions involving all the NMR-detected boron species. We assumed reversible exchange reactions and irreversible hydrolysis reactions on the grounds of the corresponding thermodynamic parameters. In fact, whereas the hydrolysis is a strongly favored process (Gibbs free energy variation, $\Delta G = -320$ kJ mol^{-1}), the free energy of any H/D exchange process is expected to be near zero. Ab initio calculations on the relevant chemical species involved in such reactions (Table 3) allowed us to generate thermochemical information, such as reaction enthalpies and Gibbs free energies. In the last column of Table 3 is reported the sum of electronic and thermal enthalpies and the sum of electronic and thermal Gibbs free energies for every minimized chemical species.

The adequacy of our theoretical approach is granted by the comparison of the calculated standard free energy (−277 kJ mol^{-1}) of the hydrolysis reaction $BH_4^- + 4H_2O \rightarrow B(OH)_4^- + 4H_2$ with its experimental value (−320 kJ mol^{-1}) if we take into account that calculations are referred to a virtual process occurring in a pure gas phase. If we compare the calculated zero-point energy difference (an observable not significantly affected by solvent interactions) at $T = 298$ K between H_2O and D_2O (15 kJ mol^{-1}) with the reported experimental value (14.9 kJ mol^{-1}), the agreement is far better. Since the H/D exchange mechanism plays a main role in the BH_4^-/D_2O system and no experimental data, to the best of our knowledge, are reported on the thermodynamic parameters of deuterium scrambling of borohydride, we decided to calculate them for every process of the type $BH_{4-n}D_n^- + D_2O = BH_{3-n}D_{n+1}^- + HDO$ with $n = (0, 1, 2, 3)$. As we can appreciate in Table 3, since the calculated ZPE difference between $BH_{4-n}D_n^-$ and $BH_{3-n}D_{n+1}^-$ is lower than the calculated ZPE difference between D_2O and HDO, the calculated Gibbs free energy of all the above processes is slightly positive (about +2.5 kJ mol^{-1}). At $T = 298$ K, $K_{eq,exc}$, the associated thermodynamic equilibrium constant would be therefore just a little less than 1 (about 0.4) when all the products and reactants are at their standard concentration (1.0 M). The equilibrium position is expected to be strongly shifted toward the products (deuterated hydrides) due to the initial conditions of our reaction where the solvent, D_2O, is present in large molar excess in the reaction medium.

Moving along similar lines as those described above for the simplified reaction scheme, the solutions of the differential equations (see Supporting Information, eqs 11−19) were fitted to the NMR data (Figure 4) obtaining the "best" values of all the involved hydrolysis (k_{hyd}) and exchange rate constants ($k_{\pm i,exc}$) as reported in Table 2.

These results confirm those already outlined in the simplified model; thus, exchange rate constants are again higher (in particular, those relative to the backward processes) than hydrolytic rate constants and indicate a slight decrease of both exchange and hydrolytic rate constants with the increase of deuterium content on the reaction intermediates. The only exception is represented by the rate constants of the processes

TABLE 3: Absolute Energies (*E*s) and ZPEs at 298 K Scaled by 0.98 at DFT-B3LYP/6-311++G(d,p) Level

molecular species	E^a [au]	zero-point correction [kJ mol^{-1}]	ΔZPE [kJ mol^{-1}]	$\Delta H°$ sum of electronic and thermal enthalpies [au]	ΔG° sum of electronic and thermal free energies [au]
BH_4^-	−27.275299	90.9	0.0	−27.238204	−27.259688
BH_3D^-		85.8	5.1	−27.240301	−27.262218
$BH_2D_2^-$		80.4	10.5	−27.242426	−27.264758
BHD_3^-		74.9	16.0	−27.244576	−27.267308
BD_4^-		70.8	20.1	−27.246752	−27.269868
H_2O	−76.458531	62.0	0.0	−76.433014	−76.453267
HDO		54.4	7.6	−76.435936	−76.457911
D_2O		46.9	15.1	−76.438903	−76.46104
$B(OH)_4^-$	−328.486674	167.9	0.0	−328.419188	−328.453355
$B(OD)_4^-$		136.9	31.0	−328.431426	−328.467169
H_2	−1.1795715	33.1	0.0	−1.166414	−1.181200
HD		31.0	4.2	−1.167733	−1.183364
D_2		26.8	6.3	−1.169297	−1.185718
BH_3OH^-	−102.561549	116.0	0.0	−102.516417	−102.544083
BD_3OD^-		90.4	25.6	−102.526176	−102.555328
BO_2^-	−175.521600	31.4	0.0	−175.508277	−175.53344

[a] 1 au = 2624 kJ mol^{-1}.

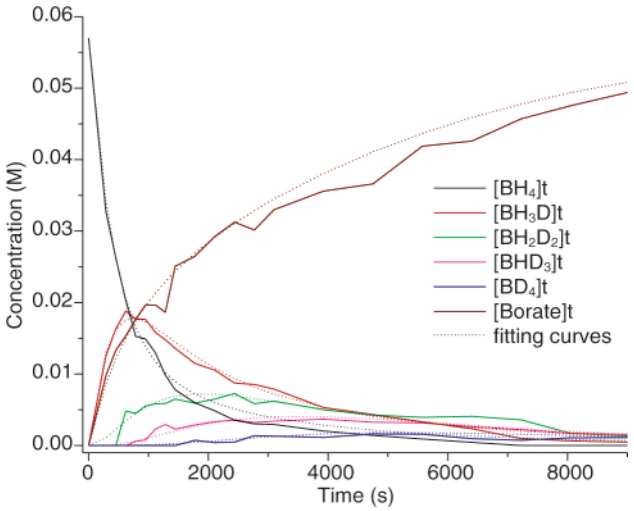

Figure 4. Optimized model. Dashed lines: fitting curves. Solid lines: experimental data.

involving the BD_4^- species, but our experimental NMR measurements do not allow us to obtain reliable values, since its NMR signal was not significantly higher than the instrumental noise. Therefore, the values of such rate coefficients ($k_{8,exc}$, $k_{-8,exc}$, and $k_{9,hyd}$ reported in Table 2) can be considered just indicative estimates.

3.2.3. NMR Kinetics Measurements with $NaBD_4$ in Alkaline H_2O and in D_2O. Deuterium/hydrogen exchange was also observed when the reaction was carried out in solution 3. However, using $NaBD_4$, the initial multiplet extends over so wide a frequency domain (more than 100 Hz in the early part of the process) as to hinder the analysis of the single scrambled H/D hydrides $BH_nD_{4-n}^-$ ($n = 1, 2, 3, 4$); even if they appeared in the ^{11}B NMR spectra one after another, their NMR signals were heavily overlapped. Hence, the evaluation of the kinetic parameters of all the exchange processes was not practicable, but nevertheless, the hydrolytic rate constant was obtained by nonlinear least-squares regression fitting of the rate of disappearance of the overall unresolved multiplet belonging to the $BH_nD_{4-n}^-$ species and from the rate of formation of the end product borate $B(OH)_4^-$. The rate constant thus obtained was $k_{hyd}(BD_4^-/H_2O)$ $3.3 \pm 0.5) \times 10^{-3}$ s^{-1} M^{-2}, which is about the same as the above-discussed $k_{hyd}(BH_4^-/H_2O)$. In such a system, the $t_{1/2}$ was estimated by the crossing point between hydrides and borate curves to be (300 ± 10) s. Isotope effect due to B−H(D) bond breaking seems therefore not effective.

Finally, the rate constant of the BD_4^-/D_2O reacting system (solution 4) was evaluated to be $k_{hyd}(BD_4^-/D_2O) = (7.7 \pm 0.2) \times 10^{-4}$ s^{-1} M^{-2} with a $t_{1/2}$ of (1490 ± 20) s, leading to an estimated solvent isotope effect of about (4.5 ± 0.4).

3.2.4. Mechanistic Considerations. So far, we have demonstrated that the hydrolysis of sodium borohydride on Pd/C obeys the rate law $-d[NaBH_4]/dt = k_{obs}[BH_4^-]$, with an activation energy of 28.5 kJ mol^{-1}. Moreover, the observed rate constant for the hydrolysis of the corresponding perdeuterated analogue BD_4^- in H_2O has been found, within experimental error, to assume the same value as that of BH_4^- in H_2O. This suggests that the cleavage of the B−H bonds in all species along the reaction coordinate does not contribute to the rate-determining step. Moreover, the nondetectability in our NMR spectra of any partially hydrolyzed intermediates of the type $BH_{4-n}(OH)_n^-$ indicates that their lifetime is short on the NMR time scale. Finally, H/D exchange among $BH_nD_{4-n}^-$ ($n = 0, 1, 2, 3, 4$) has been detected both in the BH_4^-/D_2O and in the BD_4^-/H_2O reacting systems. In particular, in the former system we have highlighted through a detailed kinetic analysis and by high-level theoretical calculations a significant isotope effect on the hydrolysis. If, for the sake of reliability, we consider only the kinetic parameters of the reaction steps involved in the first half of the reaction course showed in Figure 4, it is evident that (i) the hydrolytic rate constant in D_2O of the starting BH_4^- species, 1.3×10^{-3} s^{-1} M^{-2}, is about one-third of the corresponding rate constant in H_2O, and the major contribution to BH_4^- disappearance is given by the forward exchange process leading to BH_3D^- species; (ii) the hydrolytic rate constant of BH_3D^- in D_2O is about one-third (1.3×10^{-3} s^{-1} M^{-2}) of that of BH_4^- in the same solvent, and again, the main contribution to its disappearance is given by the forward process leading to $BH_2D_2^-$; and (iii) the exchange rate constant in the BH_3D^-/BH_2D_2 system is, in turn, about one-half of that evaluated in BH_4^-/BH_3D^- system. In our opinion, the latter outcome can be explained on statistical grounds by taking into account that deuterium incorporation can be obtained by the exchange with any one of the four H atoms in the BH_4^- species, while it occurs only by exchanging with three H of BH_3D^-, thus introducing a further activation entropy contribution into the rate constant of the latter reaction. It must be emphasized that the rate of D−H exchange in acid-catalyzed hydrolysis of BH_4^- is much slower than the rate of hydrolysis, as demonstrated by hydrolysis of BH_4^- in D_2O, or BD_4^- in H_2O, in which mainly HD (90−95%) is evolved.[27] This outcome is in sharp contrast with reactivity of $NC-BH_3^-$ and Me_3N-BH_3 wherein the rates of D−H exchange are much greater than their rates of hydrolysis being 15-fold in the case $NC-BH_3^-$[28] and even more for Me_3N-BH_3,[29] allowing the preparation of $NC-BD_3^-$ and R_3N-BD_3 derivatives by treatment of hydrogenated hydride reagents in D_3O^+/D_2O at relatively low pD values. The above examples demonstrate that any change in the coordination sphere of boron results in a dramatic change in the kinetics of both hydrolysis and D−H exchange in borohydride complexes. In the palladium-catalyzed hydrolysis discussed here, borohydride is thought to interact with the metal surface producing a surface-linked borohydride complex.

Through a reversible dissociative chemisorption of BH_4^-, palladium atoms should produce the surface intermediate species $Pd-BH_3^-$ and Pd−H hydride, as shown in Figure 5 and eqs 2−6

$$BH_4^- + 2Pd \rightleftharpoons BH_3Pd^- + PdH \quad (2)$$

$$PdH + D_2O \rightleftharpoons PdD + HDO \quad (3)$$

$$BH_3Pd^- + PdD \rightleftharpoons BH_3D^- + 2Pd \quad (4)$$

$$BH_3Pd^- + D_2O \rightarrow BH_3OD^- + PdD \quad (5)$$

$$PdH + PdD \rightarrow 2Pd + HD \quad (6)$$

Addition of the species involved in the steps in eqs 2−4 leads to the overall exchange reaction $BH_4^- + D_2O \rightleftharpoons BH_3D^- + HDO$, while considering steps 2, 5, and 6, we obtain the hydrolysis reaction $BH_4^- + D_2O \rightarrow BH_3OD^- + HD$. The intermediate $BH_3(OH)^-$ undergoes further hydrolysis with a faster rate than BH_4^- itself.

Whereas the boron atom in $Pd-BH_3^-$ undergoes irreversible reductive attack by H_2O leading to the monohydroxy borohydride BH_3OH^- and to the metal hydride Pd−H, the quenching of Pd−H affords H_2 and a free palladium active site. On the other hand, when the reaction is carried out in D_2O, the Pd−D

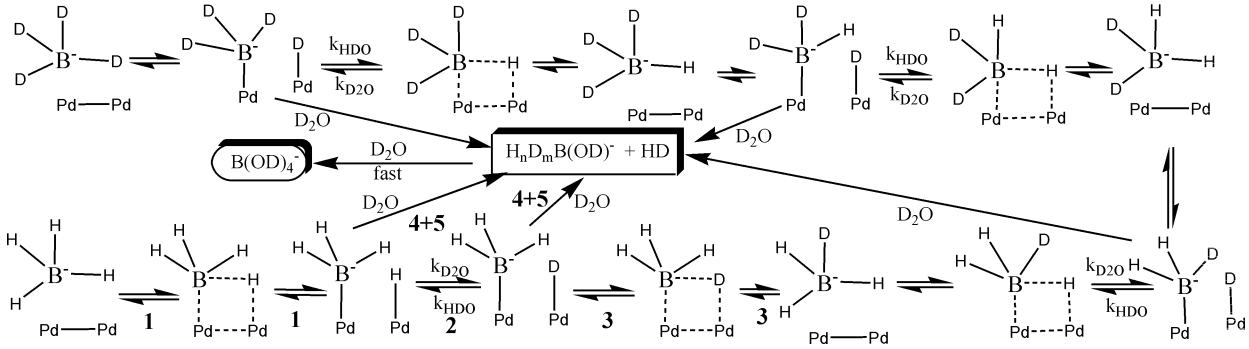

Figure 5. Proposed mechanism for the Pd-catalyzed hydrolysis of BH_4^- in D_2O. Numbers 1, 2, 3, and 4 refer to eqs 2−5.

species (that can be produced both by nucleophilic attack of the oxygen atom on the boron atom of the palladium-coordinated $PdBH_3^-$ species (eq 5) and/or by H/D exchange of D_2O (eq 3) on the PdH species) can either introduce the D isotope into the $Pd-BH_3^-$ species affording $PdBH_2D^-$ and/or lead to HD via reaction with PdH, thus regenerating the required free form of the catalyst. A primary kinetic solvent isotope effect will be observed if a proton (deuteron) is transferred from the solvent in the rate-determining step of the reaction.

Since a significant solvent isotope effect on the hydrolytic rate constant has been observed when the reaction is carried out in D_2O ($k(H_2O)/k(D_2O) \approx 4.5$), the rate-determining step must involve the breaking of the O−D bond both in the hydrolysis and in the exchange route. On the other hand, no isotope effect on the hydrolysis rate has been detected within the reacting system BD_4^-/H_2O, indicating that a fast chemisorption of the hydride into the palladium surface is occurring and that the stronger B−D bond breaking does not occur in the rate-determining step of the hydrolysis.

All this evidence seems to suggest a reaction course as showed in Figure 5 where the intermediates $PdBH_nD_n^-$ ($n + m = 3$; $n = 0, 1, 2, 3$) represent the active substrates for both the hydrolytic and exchange routes playing the same role of the neutral BH_nD_m ($m + n = 5$; $n = 0, 1, 2, 3, 4, 5$) species in the acid-catalyzed process. Since in the BH_4^-/D_2O reacting system we have observed that the H/D scrambling is faster than the corresponding hydrolytic process, the activation energy of the latter must be higher than that of the former.

A schematic energy profile for the BH_4^-/D_2O reacting system that summarizes all our data is reported in Figure 6.

The thermochemical values used to place the scrambled intermediates relative to starting BH_4^- are calculated from theoretical ab initio calculations (Table 3) as enthalpy differences. Thus, for instance, the reported +8.7 kJ mol^{-1} (endothermic process) in correspondence to BD_4^- species is the calculated thermally averaged enthalpy difference of the reaction $BH_4^- + 4D_2O \rightleftarrows BD_4^- + 4HDO$. The energy levels of other scrambled intermediates have also been placed according to the enthalpy difference value of the reactions $BH_4^- + nD_2O \rightleftarrows BH_{4-n}D_n^- + n$HDO leading to +2.1 kJ mol^{-1} (BH_3D^- + HDO), 4.2 kJ mol^{-1} ($BH_2D_2^-$ + 2HDO), 6.6 kJ mol^{-1} (BHD_3^- + 3HDO), and 8.7 kJ mol^{-1} (BD_4^- + 4HDO). Concerning the hydrolysis products, the same approach has been used to calculate the relative energy of BH_3OD^- (−29 kJ mol^{-1}, exothermic process) as the enthalpy difference of the reaction $BH_4^- + D_2O \rightleftarrows BH_3OD^- + HD$ and of the end products $B(OD)_4^-$ (−292 kJ mol^{-1}) as the enthalpy difference of the overall hydrolytic reaction $BH_4^- + 4D_2O \rightleftarrows B(OD)_4^- + 4HD$. The relative position of intermediates and transition states are instead purely hypothetical but somehow account for all kinetics observations. We believe that such a scenario has wide significance and implications for many metal-catalyzed hydrolysis of sodium borohydride and its analogues. From such an energy profile, we can appreciate that under thermodynamic constraints (for example, in the case of high temperature or low activation energy barriers) the strong exothermicity of the hydrolysis route would drive the reaction irreversibly toward borate and hydrogen evolution, whereas H/D exchange could not be observed. If, however, the reaction is carried under kinetic conditions, a fast equilibration among scrambled hydrides could occur without opening the hydrolysis channel, since the activation barrier of exchange E_a(exc) could be lower than E_a(hyd). In such conditions, it would be possible to obtain pure BD_4^- by exploiting the strong mass law effect of the deuterated solvent (D_2O). The cyanoborohydride BH_3CN^- fulfills such a requirement, and we can anticipate here that, by using the same reaction conditions as for the BH_4^-/D_2O system, no hydrolytic products, but only H/D exchanged hydrides, can be detected in ^{11}B NMR measurements of the BH_3CN^-/D_2O system. As already discussed, the Pd-catalyzed hydrolysis of BH_4^- in D_2O is far from such an extreme state; it behaves as an intermediate case affording in the reaction course both hydrolysis and exchanged products but with slightly higher rates for the exchange elementary steps.

Whatever the true mechanism, palladium hydride species are thought to play a main role both in the exchange and in the hydrolytic routes. Although the properties of transition metal hydrides have been (and are) of great interest, there is still a lack of basic information on metal−hydrogen (in particular on Pd−H) energetics. The simplest systems would be the diatomic MH molecules, which however are formed only in the gas phase and are usually transient species. By analyzing measured homolytic bond energies of such transition metal hydrides, it has been found that the average M−H bond energy is higher for metals with high electronegativity, with low promotion energy from the ground state to the reactive valence state, and with high M−M bond energy.[30] The latter is often unknown but can be estimated from the heat of metal atomization enthalpy, which represents the strength of the corresponding metal−metal bond. Following these lines, it is expected that Pd−H bond energy is lower of that of Ni−H, and even much lower than Pt−H. Another important chemical property that can be accounted for by the above-cited thermodynamic functions is the hydridic−protonic preference of a given transition metal hydride in a given solvent, for example, water. A metal hydride has a relevant hydridic character only if its electronegativity is very low, and thus, for example, the Cu−H bond is considered hydridic, whereas Au−H is essentially protonic. On these grounds, we can evaluate that, whereas the Pd−H bond is essentially hydridic (therefore, PdH + H_2O leads to reversible equilibrium with PdOH + H_2 products and PdH + D_2O to PdOD + HD through H/D exchange), Pt−H is expected to be

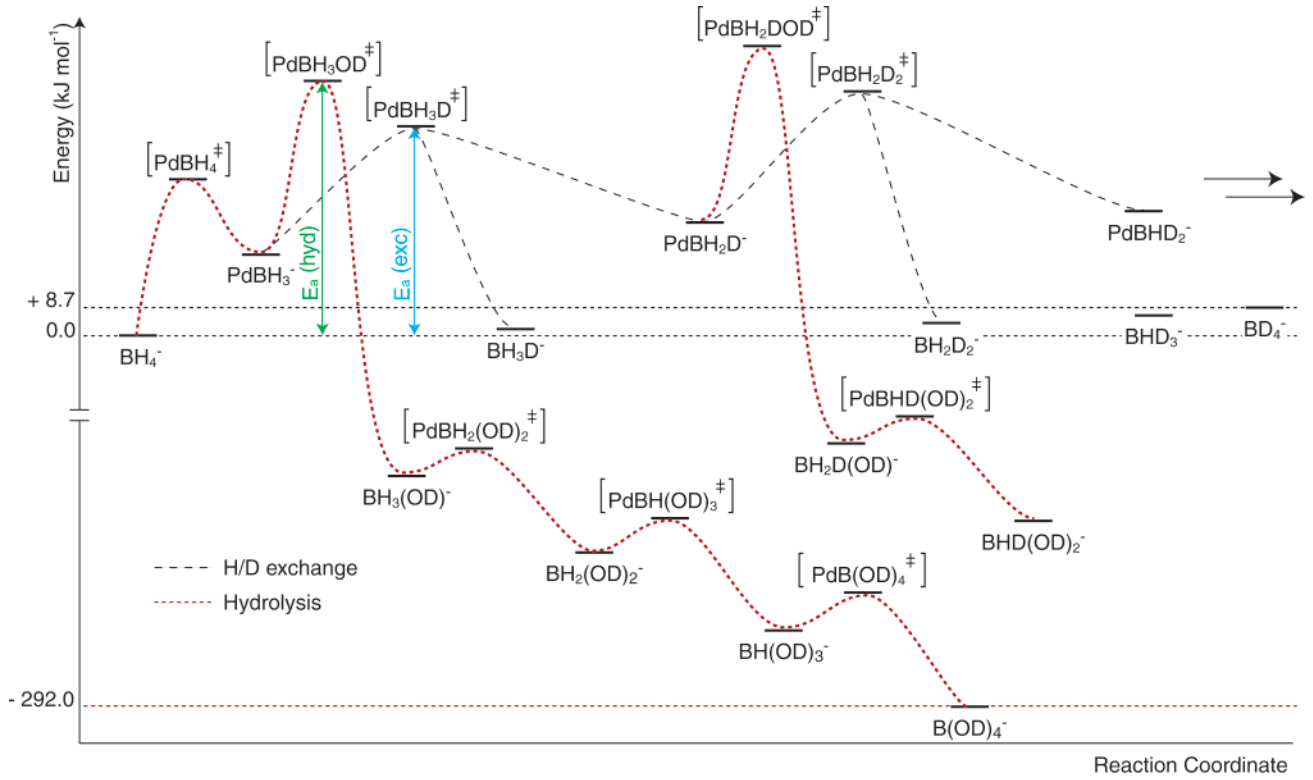

Figure 6. Schematic reaction coordinate diagram for the BH_4^-/D_2O reacting system. The thermochemical values used to locate products ($BH_nD_{4-n}^-$ + *n*HDO) relative to starting reagent BH_4^- + nD_2O are from DFT-B3LYP/6-311++G(d,p) ab initio calculations. The broken lines connecting starting materials, intermediates, transition states, and products are purely hypothetical but in agreement with all kinetic observations.

protonic due to the higher electronegativity of Pt with respect to Pd atoms. Our preliminary results on Pt/C-catalyzed hydrolysis of $NaBH_4$ not only suggest that the rate constant for the H_2 production is higher than that measured here for the Pd/C catalyst but also that the hydrolysis rate constant is at least 1 order of magnitude higher than the H/D scrambling processes. Our investigations will be focused on such a topic in the future in order to better understand the atomic/molecular aspects affecting the overall catalysis.

Conclusions

We have exploited the NMR-suitable properties of palladium atoms (low magnetic moment) in order to develop a very effective methodology for analyzing kinetics aspects of the Pd-catalyzed hydrolysis of $NaBH_4$. Such a methodology mainly relies on ^{11}B NMR on the heterogeneous mixture given by solid catalyst dispersed in the hydride's aqueous alkaline solution without recourse to any workup. In particular, $^{11}B-^{1}H$ NMR decoupled spectra acquired with Hahn spin−echo pulse sequence have been proven here to be a vast source of information on the reaction path and very useful for a complete kinetic analysis substantiated by substrate and solvent isotope effects. NMR spectra have been taken continuously during the catalytic conversion of the BH_4^- hydrogen/deuterium mixtures in order to follow the kinetics of the reaction by recording all the detected NMR signals as a function of time.

To the best of our knowledge, such an approach has never been attempted, possibly due to the common (and correct) opinion that high-resolution NMR measurements can be performed only on homogeneous samples and in the absence of paramagnetic species. As a matter of fact, we were quite surprised to realize that, at least when the metal catalyst does not possess a significant magnetic moment, not only NMR spectra with good resolution (line width in the range 2−4 Hz, whereas B−H coupling constants are about 12 Hz) but also reliable kinetic data could be obtained. We can anticipate here that such a case is not restricted to palladium-supported catalyzed reactions. It is worthy of note that the opportunity to follow the reaction course of any chemical process with NMR detection offers great advantages with respect to other analytical techniques , since it is possible to have both quantitative data and precise structural identification of eventual intermediates such as, in our case, the partially deuterated borohydride species.

By fitting the kinetics NMR data with the numerical solutions of the appropriate differential equations describing a given reaction system, we have evaluated the rate constants of the elementary steps of the palladium-catalyzed borohydride hydrolysis. Our results highlight the following: (i) $BH_{4-n}D_n^-$ but not $H_nB(OD)_{4-n}^-$ (n = 1, 2, 3) are the only long-living intermediates (at least on the NMR time scale), thus indicating that the latter undergo hydrolysis at a faster specific rate than BH_4^- itself; (ii) B−H bond cleavage does not contribute to the rate-determining step, since no substrate isotope effect can be observed; (iii) since solvent isotope effect is present, the rate-determining step must involve the breaking of the water O−H bond both in the hydrolysis and in the exchange route; and (iv) since in the BH_4^-/D_2O reacting system we have observed that the H/D scrambling is faster (at least in the early part of reaction course) than the corresponding hydrolytic process, the activation energy of the latter must be slightly higher than that involved in the exchange process.

More generally, the role played by the metal in the hydrolysis seems quite different from the role played by H^+ in the acid-catalyzed process. Whereas in the latter the H_2 (and Borax) production is induced by a rate-determining step wherein a proton attacks the boron atom to give the neutral intermediate BH_5, which in turn affords H_2 and reactive BH_3 species, in alkaline solutions the activation of the substrate toward hy-

drolysis is caused by electron-withdrawing and electron-releasing effects of the palladium atoms on the catalyst surface via the putative chemiadsorbed species $Pd-BH_3^-$ and Pd−H.

Acknowledgment. We acknowledge Damiano Avi for Micro GC measurements. This work was granted by the Department of Physics, University of Trento, in the framework of the italian hydrogen-FISR program.

Supporting Information Available: A complete description of the differential equations corresponding to each reaction scheme. This material is available free of charge via the Internet at http://pubs.acs.org.

References and Notes

(1) Latimer, W. M. *Oxidation Potentials*; Prentice-Hall: Englewood Cliffs, NJ, 1952.
(2) Morris, J. H.; Gysling, H. J.; Reed, D. *Chem. Rev.* **1985**, *85*, 51−76.
(3) Gardiner, J. A.; Collat, J. W. *J. Am. Chem. Soc.* **1965**, *87*, 1692−1700.
(4) Lyttle, D. A.; Jensen, E. H.; Struck, W. A. *Anal. Chem.* **1952**, *24*, 1843−1844.
(5) Schlesinger, H. I.; Brown, H. C.; Finholt, A. B.; Gilbreath, J. R.; Hockstra, H. R.; Hydo, E. K. *J. Am. Chem. Soc.* **1953**, *75*, 215−219.
(6) Davis, R. E.; Swain, C. G. *J. Am. Chem. Soc.* **1960**, *82*, 5949−5950.
(7) Mesmer, R. E.; Jolly, W. L. *Inorg. Chem.* **1962**, *1*, 608−612.
(8) Wang, F. T.; Jolly, W. L. *Inorg. Chem.* **1972**, *11*, 1933−1941.
(9) Davis, R. E.; Kibby, C. L. *J. Am. Chem. Soc.* **1960**, *82*, 5950−5951.
(10) Schreiner, P. R.; Schaefer, H. F., III.; Schleyer, P. v. R. *J. Chem. Phys.* **1994**, *101*, 7625−7632.
(11) Stanton, J. F.; Lipscomb, W. N.; Bartlett, R. J. *J. Am. Chem. Soc.* **1989**, *111*, 5173−5180.
(12) Tague, T. J., Jr.; Andrews, L. *J. Am. Chem. Soc.* **1994**, *116*, 4970−4976.
(13) Kreevoy, M. M.; Hutchins, J. E. C. *J. Am. Chem. Soc.* **1972**, *94*, 6371−6376.
(14) Kaufman, C. M.; Sen, B. *J. Chem. Soc., Dalton Trans.* **1985**, 307−313.
(15) Holbrook, K. A.; Twist, P. J. *J. Chem. Soc. A* **1971**, *15*, 890−894.
(16) Rance, M.; Byrd, R. A. *J. Magn. Reson.* **1983**, *52*, 221−240.
(17) Cobas, J. C.; Sardina, F. J. *Concepts Magn. Reson.* **2003**, *19A*, 80−96.
(18) Mendes, P. *Comput. Appl. Biosci.* **1993**, *9*, 563−571.
(19) Mendes, P. *Trends Biochem. Sci.* **1997**, *22*, 361−363.
(20) Mendes, P.; Kell, D. B. *Bioinformatics* **1998**, *14*, 869−883.
(21) Frisch, M. J.; Trucks, G. W.; Schlegel, H. B.; Scuseria, G. E.; Robb, M. A.; Cheeseman, J. R.; Montgomery, J. A., Jr.; Vreven, T.; Kudin, K. N.; Burant, J. C.; Millam, J. M.; Iyengar, S. S.; Tomasi, J.; Barone, V.; Mennucci, B.; Cossi, M.; Scalmani, G.; Rega, N.; Petersson, G. A.; Nakatsuji, H.; Hada, M.; Ehara, M.; Toyota, K.; Fukuda, R.; Hasegawa, J.; Ishida, M.; Nakajima, T.; Honda, Y.; Kitao, O.; Nakai, H.; Klene, M.; Li, X.; Knox, J. E.; Hratchian, H. P.; Cross, J. B.; Bakken, V.; Adamo, C.; Jaramillo, J.; Gomperts, R.; Stratmann, R. E.; Yazyev, O.; Austin, A. J.; Cammi, R.; Pomelli, C.; Ochterski, J. W.; Ayala, P. Y.; Morokuma, K.; Voth, G. A.; Salvador, P.; Dannenberg, J. J.; Zakrzewski, V. G.; Dapprich, S.; Daniels, A. D.; Strain, M. C.; Farkas, O.; Malick, D. K.; Rabuck, A. D.; Raghavachari, K.; Foresman, J. B.; Ortiz, J. V.; Cui, Q.; Baboul, A. G.; Clifford, S.; Cioslowski, J.; Stefanov, B. B.; Liu, G.; Liashenko, A.; Piskorz, P.; Komaromi, I.; Martin, R. L.; Fox, D. J.; Keith, T.; Al-Laham, M. A.; Peng, C. Y.; Nanayakkara, A.; Challacombe, M.; Gill, P. M. W.; Johnson, B.; Chen, W.; Wong, M. W.; Gonzalez, C.; Pople, J. A. *Gaussian 03*, revision C.02; Gaussian, Inc.: Wallingford, CT, 2004.
(22) Lee, C.; Yang, W.; Parr, R. G. *Phys. Rev. B* **1988**, *37*, 785−789.
(23) Krishnan, R.; Binkley, J. S.; Seeger, R.; Pople, J. A. *J. Chem. Phys.* **1980**, *72*, 650−654.
(24) Amendola, S. C.; Onnerud, P.; Kelly, M. T.; Petillo, P. J.; Sharp-Goldman, S. L.; Binder, M. *J. Power Sources* **2000**, *85*, 186−189.
(25) Ozkar, S.; Zahmakiran, M. *J. Alloys Compd.* **2005**, *404*−*406*, 728−731.
(26) Kobayashi, M. *Annu. Rep. Res. React. Inst., Kyoto Univ.* **1990**, *23*, 188.
(27) Mesmer, R. E.; Jolly, W. L. *J. Am. Chem. Soc.* **1962**, *84*, 2039−2042.
(28) Kreevoy, M. M.; Hutchins, J. E. C. *J. Am. Chem. Soc.* **1969**, *91*, 4329−4330.
(29) Davis, R. E.; Brown, A. E.; Hopmann, R. P.; Kibby, C. L. *J. Am. Chem. Soc.* **1963**, *85*, 487−487.
(30) Matcha, R. L. *J. Am. Chem. Soc.* **1983**, *105*, 4859−4862.